separations

MDPI

Article

Biomass *Zilla spinosa* Fruit Functionnalized Polyethyleneimine Polymer: Analysis and Application for the Elimination of Calmagite in Water

Mahjoub Jabli [1,2,*], Arwa Elaissi [2] and Afnan Altwala [1,*]

[1] Department of Chemistry, College of Science Al-Zulfi, Majmaah University, Al-Majmaah 11952, Saudi Arabia
[2] Textile Materials and Processes Research Unit, Tunisia National Engineering School of Monastir, University of Monastir, Monastir 5035, Tunisia; elaisiarwa@gmail.com
* Correspondence: m.jabli@mu.edu.sa (M.J.); a.altwalah@mu.edu.sa (A.A.)

Abstract: The valorization of natural polymeric substrates has increased due to their uses and applications in several fields. The existence of many functional groups in their chemical structures allows them to be easily subjected to chemical modifications. This work focuses on the exploration of a new low-cost and abundant cellulosic biomass, *Zilla spinosa* fruit. The biomaterial was functionnalized with polyethyleneimine (1%, 3%, 5%, and 8%) in order to impart new reactive sites on its surface. The virgin and functionnalized biomaterials were analysed using several analytical methods; X-ray Photoelectron Spectroscopy (XPS), Fourier Transform Infrared (FT-IR), Scanning Electron Microscopy (SEM), and Thermogravimetric analysis (TGA). XPS spectrum of *Zilla spinosa*-polyethyleneimine exhibited the appearance of a new peak at 399 eV, which corresponds to N1s (5.07%). The adsorption characteristics of the prepared adsorbents were evaluated toward calmagite, an azoic and anionic dye. The adsorption capacity of *Zilla spinosa*-polyethyleneimine (5%) reached 114 mg/g at pH = 5, T = 20 °C, and time = 60 min conditions; though, it does not exceed 8.4 mg/g for the virgin *Zilla spinosa* under the same experimental conditions. The kinetic data followed both pseudo-first-order and pseudo-second-order kinetic equations suggesting a physicochemical process. The adsorption mechanism was found to be exothermic and non-spontaneous. Overall, *Zilla spinosa*-polyethyleneimine has demonstrated a high adsorption level which could be considered a promising candidate to remove synthetic dye molecules from contaminated water.

Keywords: *Zilla spinosa*; polyethyleneimine; X-ray photoelectron spectroscopy; adsorption; calmagite

Citation: Jabli, M.; Elaissi, A.; Altwala, A. Biomass *Zilla spinosa* Fruit Functionnalized Polyethyleneimine Polymer: Analysis and Application for the Elimination of Calmagite in Water. *Separations* **2023**, *10*, 296. https://doi.org/10.3390/separations10050296

Academic Editors: Xiyan Xu, Tao Duan, Dongxiang Zhang and Anwei Chen

Received: 10 March 2023
Revised: 16 April 2023
Accepted: 24 April 2023
Published: 6 May 2023

1. Introduction

Inorganic and organic pollutants could be present in the environment in different amounts due to daily human and industrial activities. These pollutants are known for their particular toxic effect on human and aquatic systems. Indeed, most of them are resistant to light, digestion, and they are carcinogenic. For these reasons, researchers throughout the world attempted to develop and design several techniques which are mainly efficient, facile to adopt, and economical in order to remove such pollutants. Numerous studies have focalized on the use and application of biomaterials and their composites for the removal of various kinds of pollutants from water, including synthetic dye molecules and toxic metals [1–8]. These studied substrates are essentially derived from agricultural and non-agricultural sources, which are naturally abundant, low-priced, and easy to manipulate. The cellulose polymer is present in several parts of the agricultural products, mainly in the leaves, shells, fibers, stems, fruits, etc. Cellulose, an important, biodegradable, cheap, and eco-friendly biopolymer, has many functional hydroxyl groups in its chemical structure. The chemical functionalization of cellulose was investigated, and it could be achieved using several reagents [9–16].

In this sense, the literature showed that many studies were carried out and reported the introduction of new functional groups onto the cellulose backbone in attempts to increase the adsorption characteristics of the biopolymer toward various pollutants. For instance, cellulose was modified with guanidinium and successfully used to remove acid fuschin (63.25 mg/g) and methyl orange (120.4 mg/g) [10]. Another study reported the amino-functionalization of cellulose using tri-ethylene tetra-amine, tri-ethylamine hydrochloride, and di-ethylene tri-amine. The adsorption capacities of the resulting products toward Reactive black 5 and Acid black 194 ranged from 117 mg/g to 150 mg/g [11]. Another work reported on the grafting of 4-vinylbenzenesulfonic acid sodium salt onto cellulose for the adsorption of Basic Red 29 (320 mg/g) [12]. In another study, an acid-functionalized coconut shell was prepared using sulfuric acid and used for the removal of methylene blue from an aqueous environment. The maximum adsorption capacity of the prepared adsorbent was equal to 50.6 mg/g at room temperature [13]. In summary, the functionalization of cellulose is accessible via different chemical methods, and it can significantly improve the adsorption characteristics of the biopolymer.

For example, we have previously investigated the extraction and the functionalization of cellulose from *Aegagropila Linnaei* using a co-polymer of dimethyl diallyl ammonium chloride and diallylamin. The prepared adsorbent displayed a high adsorption level for Acid Blue 25 (139 mg/g) [14]. We have also studied the modification of *Nerium oleander* and *Populus tremula* fibers with ethylene-diamine and hydrazine. The substrates modified with ethylene-diamine exhibited adsorption capacities for Acid Blue 161 and Acid Blue 25, equal to 35 mg/g and 67 mg/g, respectively [15,16].

Zilla spinosa grows naturally in the Sahara–Arabian deserts of North Africa in the Middle East and the north-to-central Arabian Peninsula. It originates from arid regions and is mainly adapted to desert climates. Its height reaches 60 cm. It is nearly leafless, dense-growing, and round in shape, similar to a shrub. The color of the flowers is pale blue to pale violet and develops 5-mm seedpods. *Zilla spinosa* was seldom studied in the literature, and only a few works focusing on the investigation of some of its chemical features have been carried out [17,18]. In the current work, we propose to evaluate the adsorption properties of a biomass *Zilla spinosa* fruit toward calmagite dye (a model of anionic dyes) after its functionalization with polyethyleneimine polymer at various contents (1%, 3%, 5%, and 8%). The studied materials were analysed using several analytical methods, including FT-IR, SEM, XPS, and TGA. The adsorption process was assessed under the change of several experimental conditions such as pH, time, initial calmagite concentration, and temperature. Theoretical kinetic and isotherm equations were used to better understand the behavior of the adsorption phenomenon.

2. Experimental Section

2.1. Reagents and Materials

Polyethyleneimine (Average Mw ~750,000, average Mn ~60,000, 50 wt.% in H_2O) was purchased from Sigma Aldrich and used for *Zilla spinosa* modification. All chemicals used in this study, including HCl, NaOH, etc., are of pure grade and are handled without any additional purification. Calmagite, with a molecular weight of 358.4 g/mol and chemical formula $C_{17}H_{14}N_2O_5S$, was supplied from Sigma-Aldrich in salt form and used as an adsorbate model. Deionized water was used to prepare aqueous solutions. Figure 1 gives the chemical structures of polyethyleneimine polymer and calmagite dye.

2.2. Preparation of Zilla spinosa-Polyethyleneimine

Zilla spinosa fruit (Figure 2) was collected during the period of May–June from the region of Al-Zulfi-Riyadh (KSA). In attempting to eliminate the impurities, including sand and debris, which adhere to the biomass surface, the collected *Zilla spinosa* fruit was thoroughly washed using water and dried in an oven at a temperature of 70 °C for 24 h. Further, the fruits were ground into small powders using an electrical grinder, washed again with purified water, and, lastly, oven-dried.

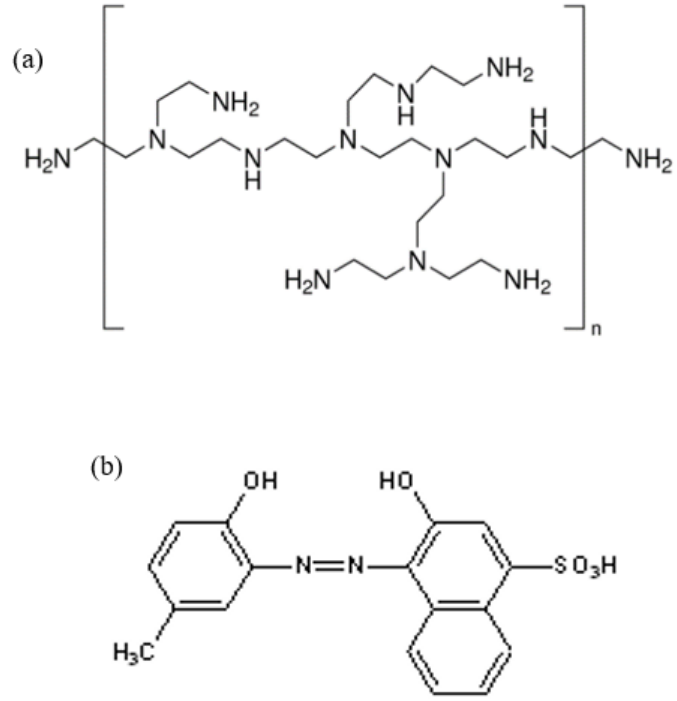

Figure 1. Structures of: (**a**) polyethyleneimine polymer and (**b**) calmagite molecule.

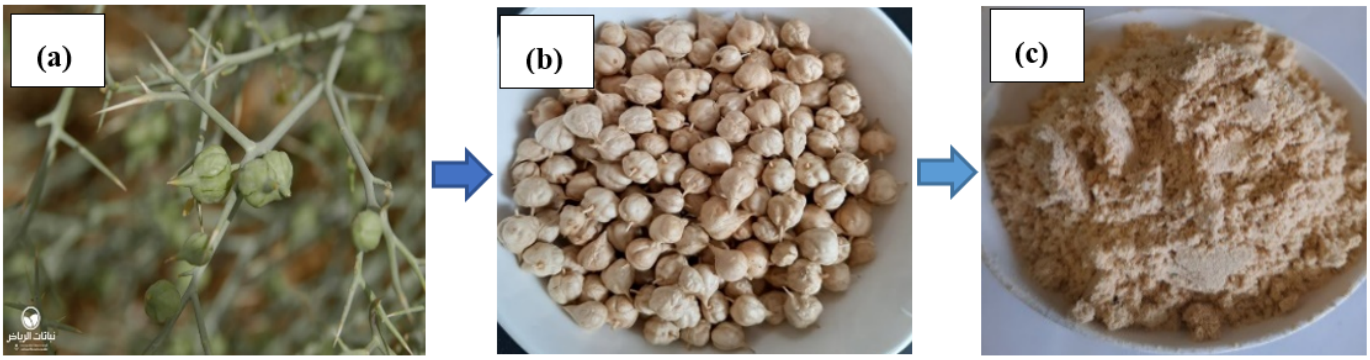

Figure 2. Photographs showing (**a**) fresh *Zilla spinosa* fruit, (**b**) dried and mature fruit, and (**c**) ground fruit.

To impart functional amino groups on the *Zilla spinosa* fruit surface, the biomass was impregnated in a solution of polyethyleneimine, which was already dissolved in demineralized water at the following percentages: 1, 3, 5, and 8 % v/v. The solution was heated at a temperature of 50 °C during a contact time of 40 min under a constant stirring speed (150 rpm). Finally, the modified *Zilla spinosa* samples were dried at 60 °C for 12 h and used as an adsorbent of anionic dyes from synthetic dye solution (herein, calmagite is used as a model of acid dyes).

2.3. Characterization

FT-IR results were acquired using a Perkin Elmer model. An apparatus of SEM Hitachi S-2360N was used to observe the morphological characteristics of the studied adsorbents. Au was used to coat the *Zilla spinosa* samples by means of a vacuum sputter-coater using an accelerating voltage equal to 20 kv. X-ray Photoelectron Spectroscopy equipped with an Al-Kα X-ray source (1361 eV) was used to analyze the surface chemistry on a Thermo ESCALAB 250XI X-ray photoelectron spectrometer (Thermo Fisher Scientific, Waltham, MA, USA). The thermogravimetric analysis (TGA) of the samples was investigated in air flow at a heating level of 10°/min using an equipment NETZSCH STA 449F3.

2.4. Adsorption Experiments

Batch adsorption experiments were carried out in Erlenmeyer flasks containing 20 mL of calmagite solution and 0.01 g of powdered *Zilla spinosa* fruit. The experimental parameters influencing the adsorption process, such as pH, contact time, initial calmagite concentration, and temperature, were examined. The absorbance of calmagite was measured at the maximum wavelength of the dye (528 nm) by using a UV-visible spectrophotometer with a typical calibration curve.

The adsorbed amount of calmagite onto the adsorbent surface was calculated using the Equation (1):

$$q(\mathrm{mg/g}) = \frac{(\mathrm{C0} - \mathrm{Ce})}{\mathrm{m}} \times \mathrm{V} \quad (1)$$

where C0 is the calmagite concentration at the initial time, Ce is the residual calmagite solution, V is the volume of calmagite used for the experiment, and m represents the mass of virgin *Zilla spinosa* or functionalized biomass used during adsorption.

3. Results and Discussion

3.1. FT-IR Spectroscopy Analysis

Figure 3 gives the FT-IR spectra of raw *Zilla spinosa* and *Zilla spinosa*-polyethyleneimine. The absorption peaks observed for the FT-IR spectrum of virgin *Zilla spinosa* prove the cellulosic structure of the studied biomass. Indeed, the absorption peak at 3337 cm^{-1} is assigned to the hydroxyl stretching groups. The absorption peaks seen at 2924 cm^{-1} and 2854 cm^{-1} confirm the existence of C–H stretching of $–CH_3$ and $–CH_2$ groups, respectively [19,20]. The peak at 1747 cm^{-1} corresponds to the C=O group of hemicelluloses [19,20]. The absorption peak at 1508 cm^{-1} could be attributed to the stretching vibrations of C=C aromatic groups in lignin [21,22]. The peak observed at 1319 cm^{-1} corresponds to the angular deformation of –CH groups in hemicelluloses [22]. The peak at 1030 cm^{-1} could be assigned to either C–O symmetric or asymmetric stretching vibration (–C–O–C– ring) of cellulose. The peak at 899 cm^{-1} is assigned to the out-of-plane angular deformation of –CH groups in the substituted aromatic rings [23]. Globally, the FT-IR absorption peaks indicate that *Zilla spinosa* contains massive oxygenous groups on its surface. Regarding the FT-IR spectrum of *Zilla spinosa*-polyethyleneimine, no significant changes are observed. However, the position of the hydroxyl groups shifted from 3337 cm^{-1} to 3325 cm^{-1}, which suggests that the hydroxyl groups of cellulose interacted with the amino groups of polyethyleneimine through hydrogen bonding or electrostatic interactions.

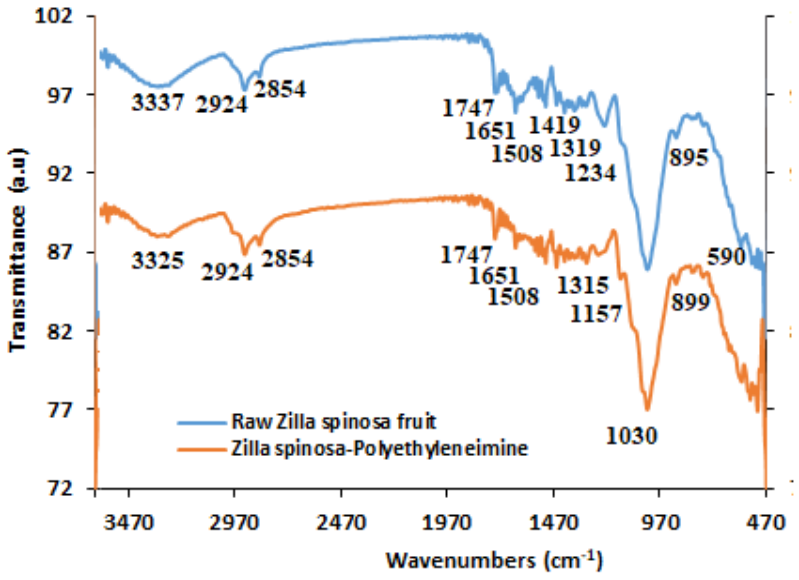

Figure 3. FT-IR spectrum of raw *Zilla spinosa* and *Zilla spinosa*-polyethyleneimine.

3.2. SEM Analysis

The SEM images of raw *Zilla spinosa* and *Zilla spinosa*-polyethyleneimine are shown in Figure 4 and observed at different magnifications (×100 and ×1000). As seen from these images, the particles exhibit irregular shapes, and no significant difference in surface roughness is observed for the unmodified and modified samples. However, the *Zilla spinosa*-polyethyleneimine sample appears clearer compared with the raw sample. The remarkable difference in color may indicate that the *Zilla spinosa* surface is homogenously functionalized with the polymer of polyethyleneimine.

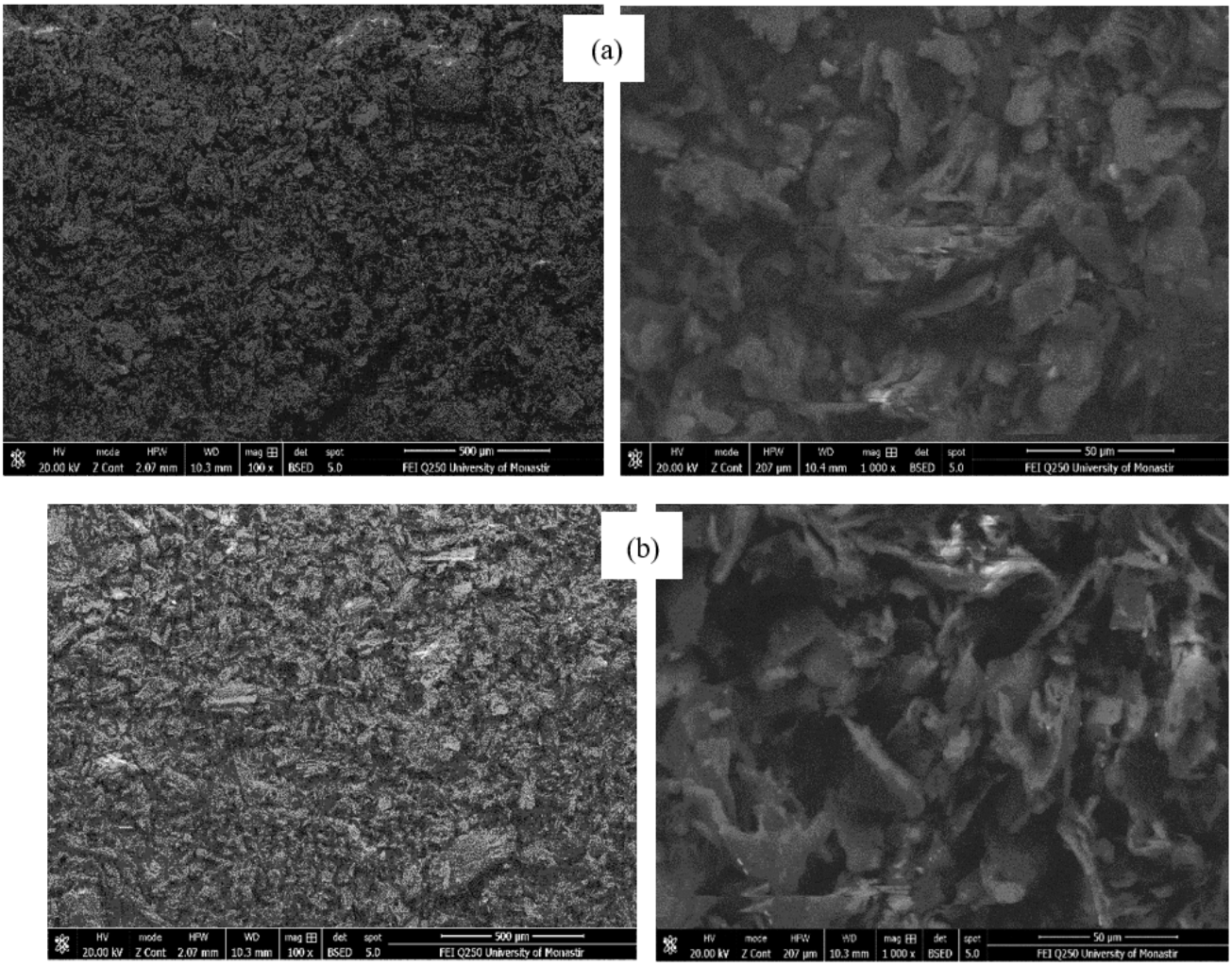

Figure 4. SEM images of: (**a**) raw *Zilla spinosa* and (**b**) *Zilla spinosa*-polyethyleneimine (×100 and ×1000).

3.3. XPS Analysis

XPS analysis is used to investigate the changes in the composition of the *Zilla spinosa* surface after chemical modification. The survey spectra of virgin *Zilla spinosa* and *Zilla spinosa*-polyethyleneimine are shown in Figure 5. According to the survey spectra, C1s and O1s peaks are seen, for virgin *Zilla spinosa*, at 285 eV and 533 eV, respectively, with the respective compositions of atomic concentration of 83.84% C and 9.07% O. However, the XPS spectrum of *Zilla spinosa*-polyethyleneimine clearly exhibits the appearance of a new peak at 399 eV, which corresponds to N1s (5.07%), confirming, therefore, the successful surface functionalization of *Zilla spinosa* fruit with amino groups.

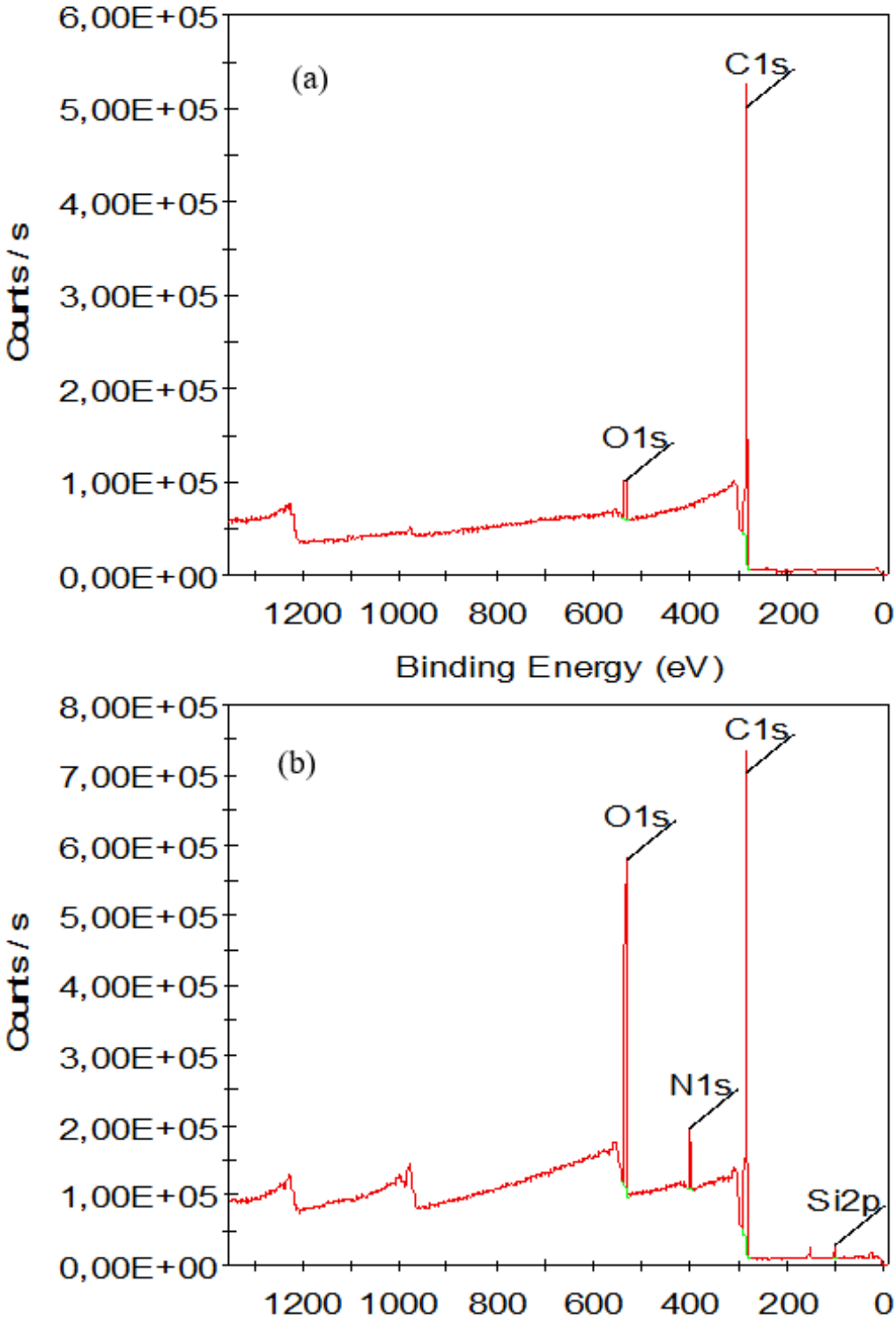

Figure 5. XPS survey of: (**a**) raw *Zilla spinosa* and (**b**) *Zilla spinosa*-polyethyleneimine.

3.4. Thermal Analysis

Figure 6 shows the TGA curves of raw *Zilla spinosa* and *Zilla spinosa*-polyethyleneimine. The analysis result reveals that the thermal degradation of cellulosic *Zilla spinosa* biomaterial occurs in several stages. During the first stage, the thermal degradation, which started at around 50 °C and ends at 94 °C, is assigned to the evaporation of water molecules from the hydrophilic sample. The weight loss at this stage is more important for functionalized biomaterial (6%) compared to the raw sample (3%). This trend can confirm

that more hydrophilic groups are added during amino-functionalization. During the second stage, the thermal event corresponds to the decomposition of cellulose and non-cellulose components. Indeed, this second decomposition includes dehydration, depolymerization, and deterioration of glycosyl cellulosic units [24,25]. At this stage, significant weight loss values are observed and are found to be equal to 57% and 52% for virgin *Zilla spinosa* and *Zilla spinosa*-polyethyleneimine, respectively. Virgin *Zilla spinosa* starts to decompose at 209 °C and ends at 342 °C. However, the thermal decomposition of *Zilla spinosa*-polyethyleneimine proceeds from 197 °C to 345 °C. The overall mass remaining values are equal to 27% and 33% for virgin *Zilla spinosa* and *Zilla spinosa*-polyethyleneimine, respectively. The chemical modification of *Zilla spinosa* with polyethyleneimine led to a reduction in the thermal stability of the biomaterial from 209 °C to 197 °C. This may be due to the occurrence of some new structural arrangements during the functionalization process.

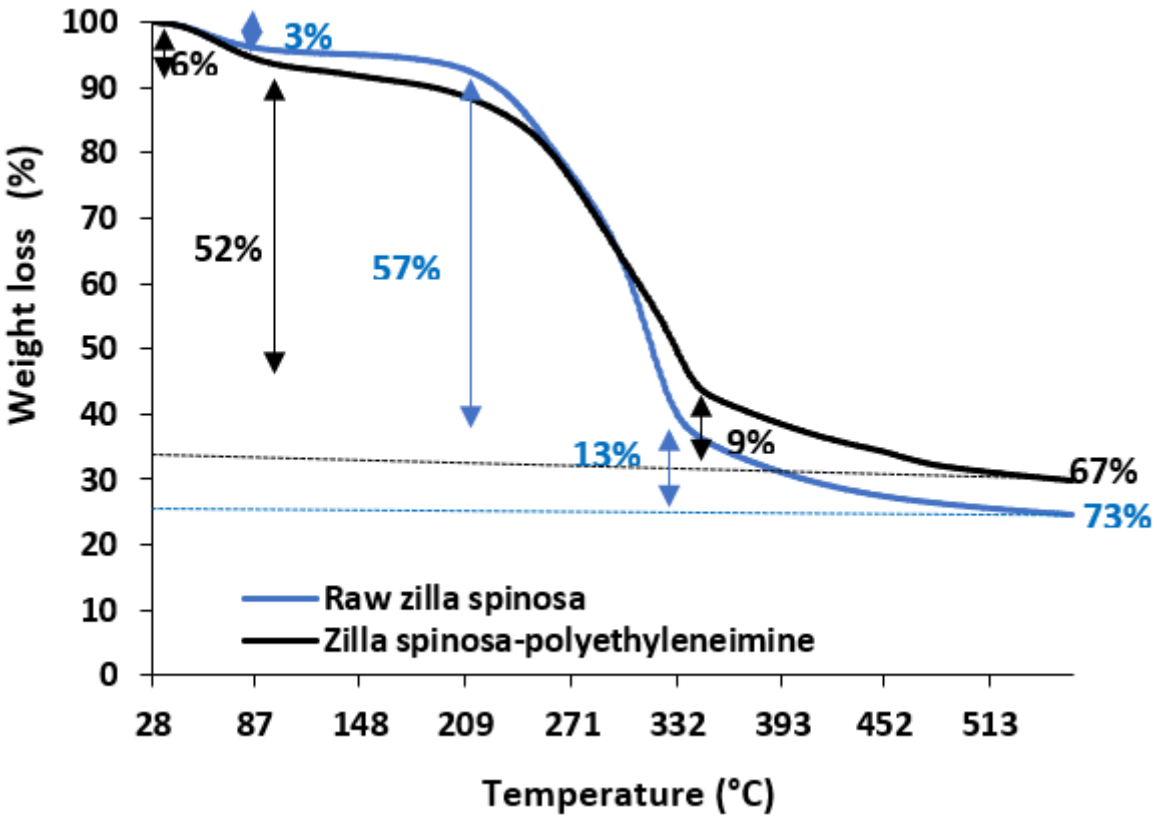

Figure 6. TGA curve of raw *Zilla spinosa* and *Zilla spinosa*-polyethyleneimine.

3.5. Application of Zilla spinosa and Zilla spinosa-Polyethyleneimine to the Adsorption of Calmagite

3.5.1. Influence of Experimental Conditions on the Adsorption Capacity

The influence of the change in initial pH, contact time, initial calmagite concentration, and temperature on the adsorption capacity was investigated in the presence of raw *Zilla spinosa* and *Zilla spinosa*-polyethyleneimine used as adsorbents. Figure 7a shows the effect of the change in polyethyleneimine content on the adsorption capacity (C0 = 30 mg/L, Time = 60 min, pH = 5, T = 20 °C). Results reveal that the adsorption capacity increases with polyethyleneimine content and achieves its maximum when the content of the polymer is equal to 5%. It is also observed that a high content of polyethyleneimine (more than 5%) lowers the adsorption capacity, which is due to the occurrence of a polymer layer on the surface of the cellulosic material or also may cause clogging of the adsorption sites.

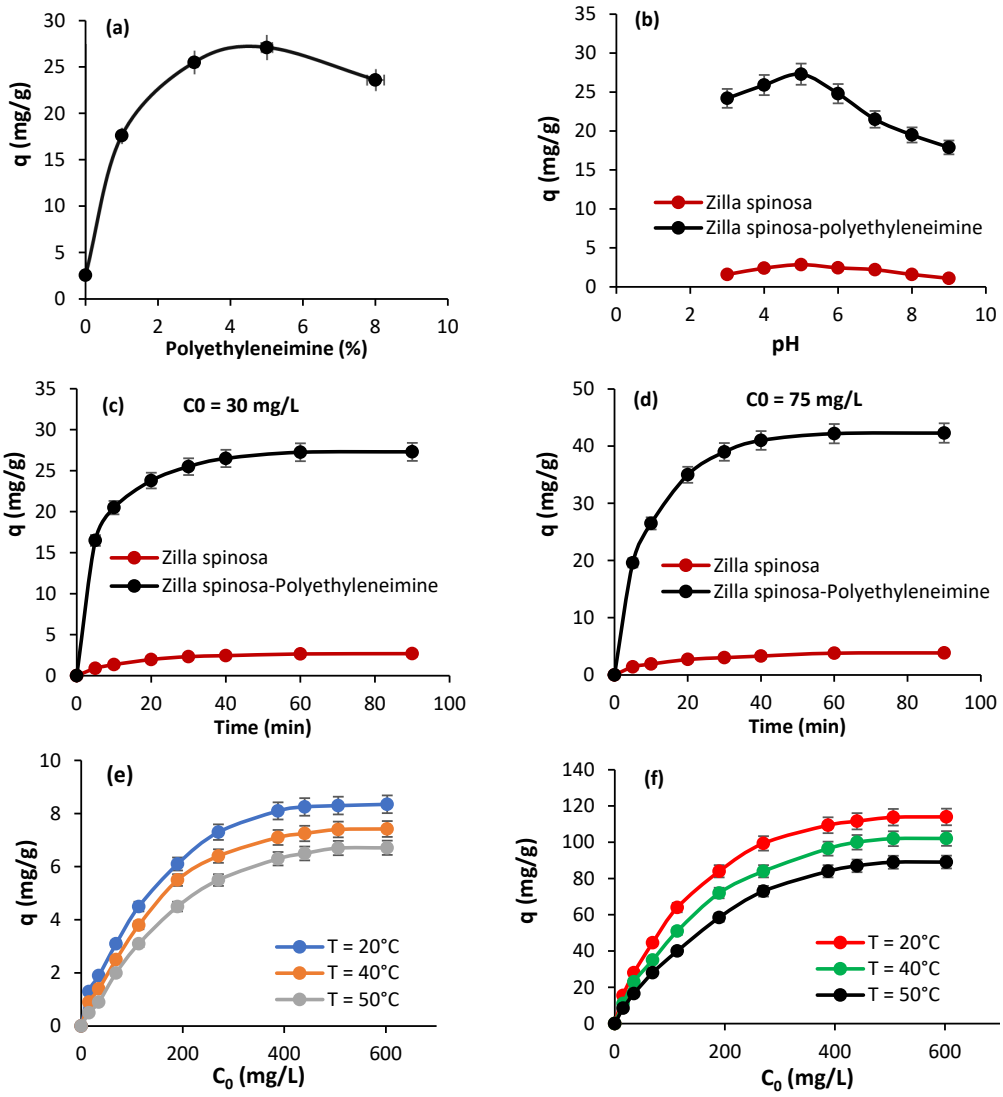

Figure 7. Effect of the experimental conditions on the adsorption capacity: (**a**) polyethyleneimine content, (**b**) initial pH variation (**c**,**d**) time change, (**e**,**f**) initial dye concentration, and temperature change.

Figure 7b gives the effect of the change in the initial pH value on the adsorption capacity of calmagite (C0 = 30 mg/L, Time = 60 min, T = 20 °C). The adsorption capacity increases with the increase in initial pH, and it reaches the maximum at pH = 5. In fact, at high acid conditions, many protons H+ are available in the solution, which favors the electrostatic attraction with the sulfonate groups of calmagite molecules. On the contrary, when the solution is alkaline, the adsorption capacity attains its minimum due to the electrostatic repulsion between the sulfonate groups of calmagite and the negative hydroxyl groups of cellulosic biomass.

The effect of time on the adsorption capacity is shown in Figure 7c,d (C0 = 30 mg/L, pH = 5, T = 20 °C). Results demonstrate that the adsorption rate of calmagite using *Zilla spinosa*-polyethyleneimine and virgin *Zilla spinosa* is rapid, and the equilibrium is approximately achieved after 60 min of contact. Regarding the obtained plots, the profile kinetic displays two important adsorption stages. From 0 min to 20 min, the adsorption is very fast, and more than 90% of the target is attained. During this stage, many adsorption sites are accessible at the adsorbent surface. Further, the adsorption continues slowly and achieves the maximum value at 60 min, which could be explained by the saturation of the active adsorption sites at this final stage of the process.

Figure 7e,f describes the effect of the variation of initial calmagite concertation and temperature on the adsorption capacity (Time = 60 min, pH = 5). Results reveal that the maximum adsorption capacities obtained using the studied adsorbents are found to be 114.6 mg/g and 8.4 mg/g for *Zilla spinosa*-polyethyleneimine and virgin *Zilla spinosa*, respectively. Indeed, the chemical modification of the cellulosic substrate with polyethyleneimine polymer meaningfully improves the adsorption capacity owing to the incorporation of many amino groups onto the cellulose backbone. However, the low adsorption capacity observed for the virgin cellulosic substrate is caused by the repulsive attraction between the negative sulfonic groups of calmagite and the negative hydroxyl groups of cellulose. Results also indicated that the adsorption process is influenced by the change in temperature value. As can be seen, the adsorption capacity of calmagite decreases with the increase in temperature, indicating an exothermic phenomenon. In the case of using *Zilla spinosa*-polyethyleneimine as an adsorbent, the adsorption level decreases from 114.6 mg/g to 89.1 mg/g when the temperature changes from 20 °C to 50 °C. However, the adsorption level is reduced from 8.4 mg/g to 6.7 mg/g in the case of virgin *Zilla spinosa* at the same temperature. This trend suggests that the interaction between the calmagite dye and the active adsorption sites present in the adsorbent surface could be weakened or broken at high temperatures and, consequently, the desorption process occurs at these particular conditions.

As observed, the adsorption capacity of calmagite depends on many experimental factors. The functional groups in the chemical structure of the studied adsorbent are also considered of great importance in adsorption. In our case, the cellulosic *Zilla spinosa* fruit can interact with polyethyleneimine through electrostatic interaction or hydrogen bonds. Indeed, the enormous hydroxyl groups present in the structure of the biomass are able to react efficiently with the reactive amino groups of polyethyleneimine in an aqueous media. The resulting complex can further react with the anionic sulfonate groups of the calmagite dye through ionic interaction or also through hydrogen bonds due to the presence of OH groups in the chemical structure of the dye (Figure 1b).

Scheme 1 gives a probable mechanism showing a possible interaction between the cellulosic biomaterial, polyethyleneimine, and calmagite.

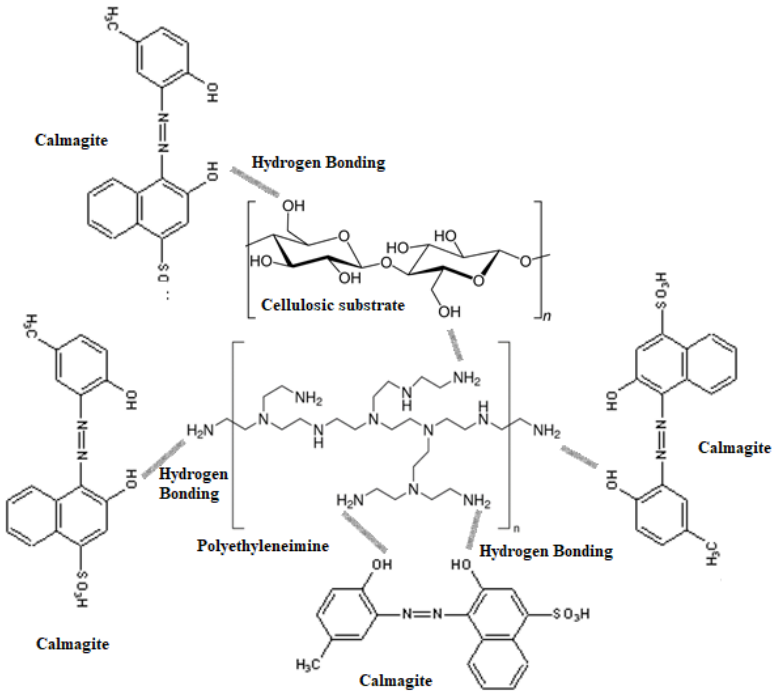

Scheme 1. A probable mechanism showing a possible interaction between the cellulosic biomaterial, polyethyleneimine, and calmagite.

3.5.2. Kinetic Study

To understand and evaluate the adsorption behavior of calmagite using *Zilla spinosa*-polyethyleneimine and virgin *Zilla spinosa* as adsorbents, the experimental data are correlated with common theoretical linear kinetic equations. Figures 8 and 9 give the plots related to the linearization results of the kinetic data. Tables 1 and 2 summarize the computed values, including correlation coefficients, constant rates, and other calculated kinetic values. The high regression coefficients ($0.98 < R^2 < 0.99$) and the consistency of the experimental adsorption capacities values with those calculated theoretically using kinetic equations, observed for both pseudo-first order and pseudo-second order, suggest a physicochemical adsorption process. Regarding the experimental data modeled through the Intra-particular diffusion kinetic equation, the corresponding plots are found to be deviated from the origin, which indicates that the adsorption phenomenon is controlled by intra-particular diffusion and also some other kinetic processes [26–28].

Table 1. Summarized kinetics, isotherms, and thermodynamic parameters related to the adsorption of calmagite on the surface of virgin *Zilla spinosa*.

Kinetic equation	Constants	Calmagite concentration (mg/L)		Isotherms	Parameters	Temperature (°C)		
		30	75			20	40	50
Pseudo first order	K_1 (min^{-1})	0.027	0.029		q_m ($mg{\cdot}g^{-1}$)	10.31	9.52	9.83
	q ($mg{\cdot}g^{-1}$)	2.57	4.34	Langmuir	K_L ($L{\cdot}g^{-1}$)	0.008	0.007	1.37
	R^2	0.99	0.98		R^2	0.99	0.99	0.97
Pseudo second order	K_2	0.03	0.018	Thermodynamic parameters	$\Delta H°$ ($KJ{\cdot}mol^{-1}$)		−5.53	
	q	3.09	4.42		$\Delta S°$ ($J{\cdot}mol^{-1}$)		−54.20	
	R^2	0.99	0.99		$\Delta G°$ ($KJ{\cdot}mol^{-1}$)	15.88	16.97	17.51
Elovich	α ($mg{\cdot}g^{-1}{\cdot}min^{-1}$)	0.93	1.27	Freundlich	K_F ($L{\cdot}g^{-1}$)	10.02	31.62	210.77
	β ($mg{\cdot}g^{-1}{\cdot}min^{-1}$)	3.44	2.40		n	1.93	1.71	1.42
	R^2	0.97	0.98		R^2	0.96	0.96	0.96
Intra-particular-Diffusion	K ($mg{\cdot}g^{-1}{\cdot}min^{1/2}$)	0.30	0.42	Temkin	b_T ($J{\cdot}mol^{-1}$)	1135	1314	1428
	R^2	0.90	0.93		A ($L{\cdot}g^{-1}$)	9.99	11.90	15.14
					R^2	0.97	0.97	0.97

Table 2. Summarized kinetics, isotherms, and thermodynamic parameters related to the adsorption of calmagite on the surface of virgin *Zilla spinosa*-polyethyleneimine.

Kinetic equation	Constants	Calmagite concentration (mg/L)		Isotherms	Parameters	Temperature (°C)		
		30	75			20	40	50
Pseudo first order	K_1 (min^{-1})	0.038	0.04		q_m ($mg{\cdot}g^{-1}$)	113.64	102.04	89.29
	q ($mg{\cdot}g^{-1}$)	20.28	43.15	Langmuir	K_L ($L{\cdot}g^{-1}$)	0.16	0.12	0.11
	R^2	0.99	0.99		R^2	0.99	0.99	0.99
Pseudo second order	K_2	0.01	0.004	Thermodynamic parameters	$\Delta H°$ ($KJ{\cdot}mol^{-1}$)		−6.09	
	q	28.57	45.87		$\Delta S°$ ($J{\cdot}mol^{-1}$)		−33.84	
					$\Delta G°$($KJ{\cdot}mol^{-1}$)	9.91	10.59	10.93
Elovich	α ($mg{\cdot}g^{-1}{\cdot}min^{-1}$)	61.61	35.43		n	2.27	2.08	1.92
	β ($mg{\cdot}g^{-1}{\cdot}min^{-1}$)	0.38	0.23		R^2	0.98	0.98	0.98
	R^2	0.94	0.94	Temkin	b_T ($J{\cdot}mol^{-1}$)	83.68	96.63	110.60
Intra-particular-Diffusion	K ($mg{\cdot}g^{-1}{\cdot}min^{1/2}$)	2.61	4.42		A ($L{\cdot}g^{-1}$)	9.75	11.70	13.59
	R^2	0.75	0.83		R^2	0.98	0.98	0.97

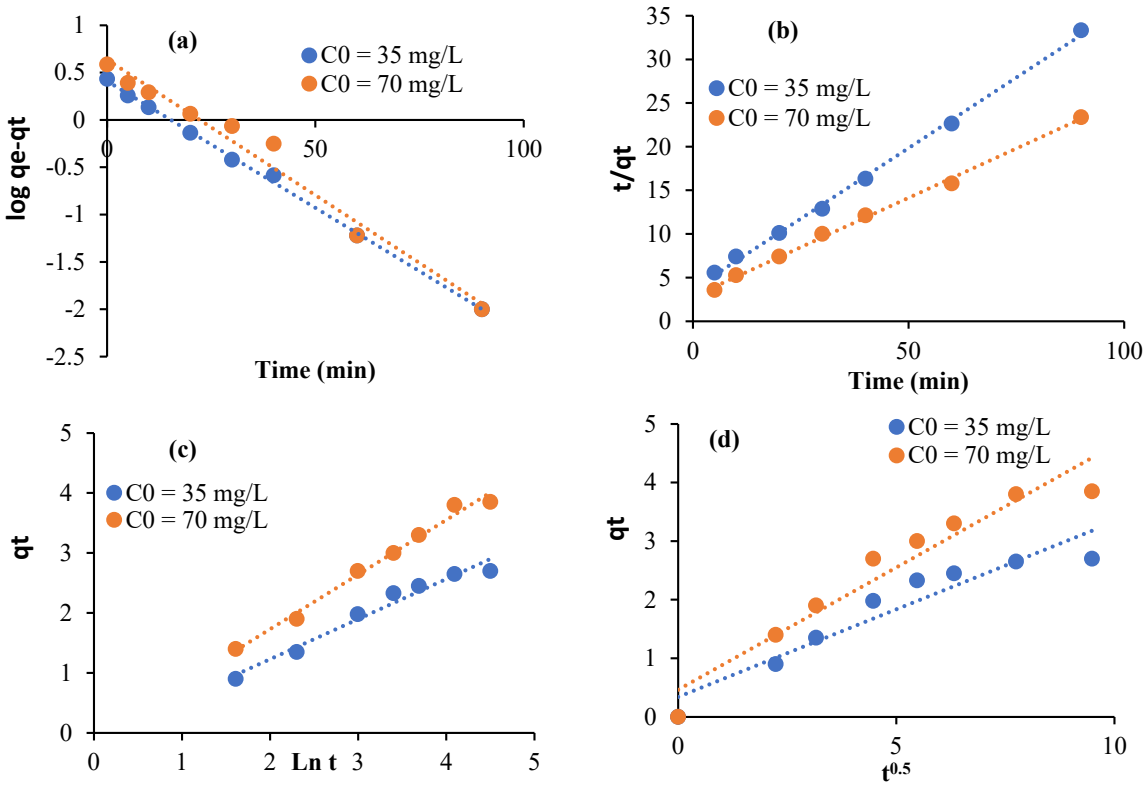

Figure 8. Kinetic plots related to the adsorption of calmagite for virgin *Zilla spinosa*: (**a**) log (qe − qt) versus time, (**b**) t/qt versus time, (**c**) qt versus Ln t, and (**d**) qt versus $t^{0.5}$.

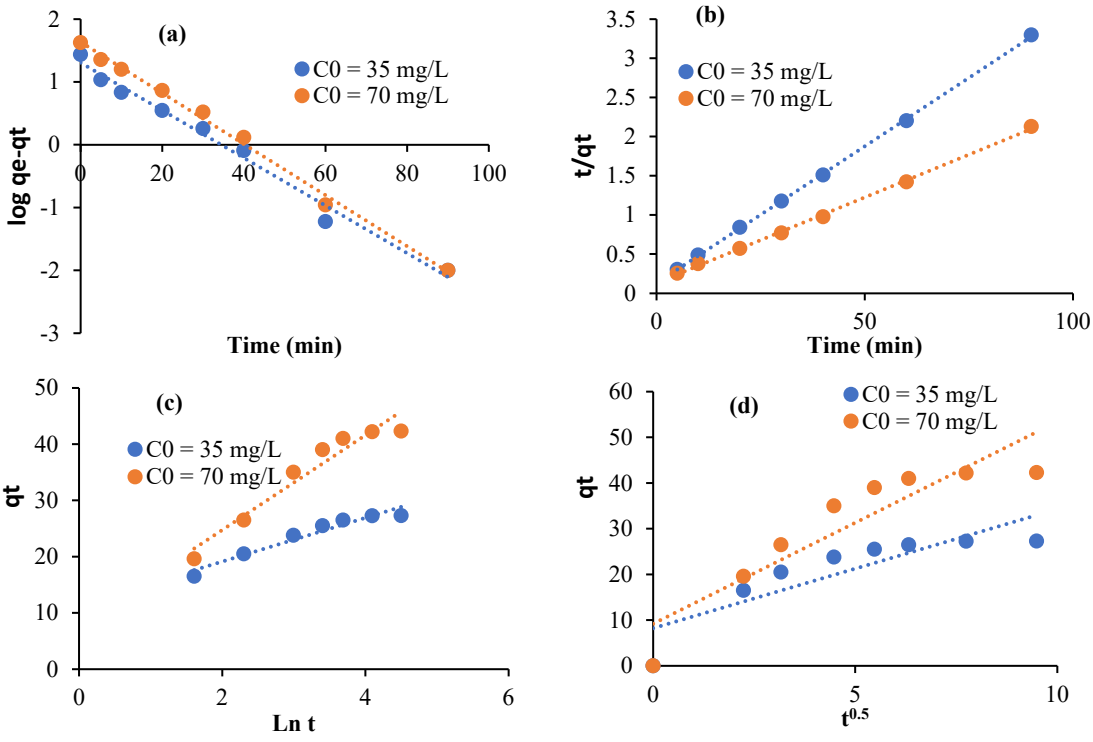

Figure 9. Kinetic plots related to the adsorption of calmagite for *Zilla spinosa*-polyethyleneimine: (**a**) log (qe − qt) versus time, (**b**) t/qt versus time, (**c**) qt versus Ln t, and (**d**) qt versus $t^{0.5}$.

3.5.3. Isotherms and Thermodynamic Study

The adsorption of calmagite using virgin *Zilla spinosa* and *Zilla spinosa*-polyethyleneimine is evaluated using Langmuir, Freundlich, and Temkin isotherms (Figures 10 and 11). The fitted parameters are itemized in Tables 1 and 2. The experimental data exhibit higher regression coefficients ($R^2 \geq 0.98$) in the case of the Langmuir model compared to other models. This behavior shows that the active adsorption sites are homogeneously distributed on the surface of the studied adsorbents, and the monolayer creation is confirmed by a straight line [29]. The parameter "n" calculated from the isotherm of Freundlich gives an idea about the favorability of the adsorption phenomenon. From the obtained results, 1 < n, which suggests that the adsorption of calmagite onto *Zilla spinosa* and *Zilla spinosa*-polyethyleneimine is favorable [30].

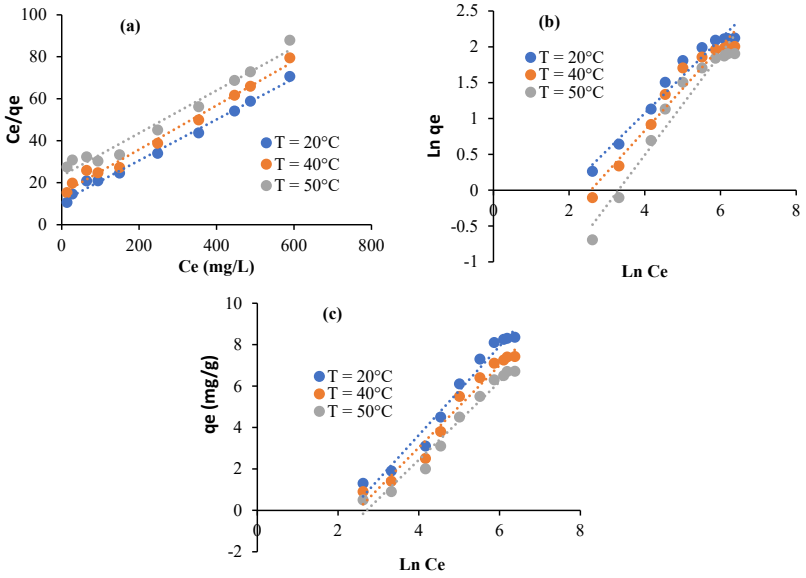

Figure 10. Isotherms plots related to the adsorption of calmagite for virgin *Zilla spinosa*: (**a**) ce/qe versus ce, (**b**) Ln qe versus Ln ce, and (**c**) qe versus Ln ce.

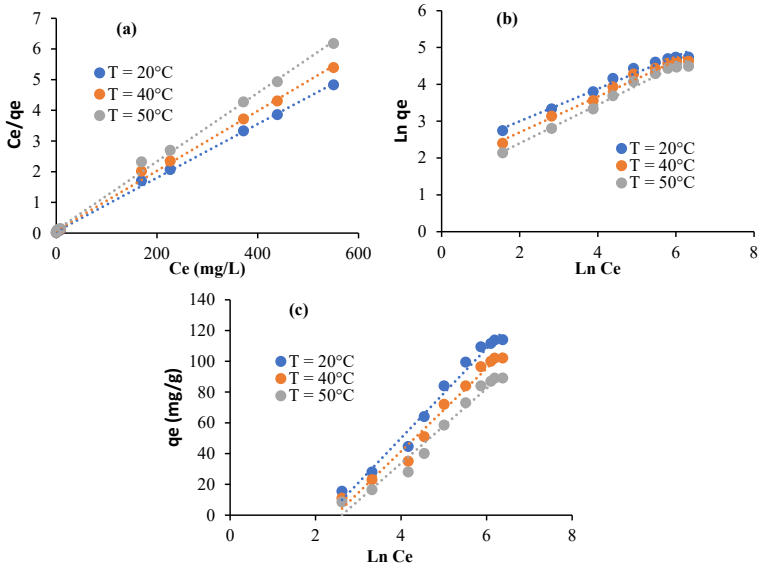

Figure 11. Isotherms plots related to the adsorption of calmagite for *Zilla spinosa*-polyethyleneimine: (**a**) ce/qe versus ce, (**b**) Ln qe versus Ln ce, and (**c**) qe versus Ln ce.

The thermodynamic parameters, such as ΔH° and ΔS°, are calculated by plotting the values of Ln (Kd) against 1/T (Figure 12). The positive value of ΔG° confirms that the adsorption of calmagite is nonspontaneous. The negative value of ΔH° proves that the interaction between *Zilla spinosa*, *Zilla spinosa*-polyethyleneimine, and calmagite is exothermic. This trend agrees well with the decrease of the adsorption capacity of calmagite with increasing temperature. The negative values of ΔS° reveal the reduction of the disorder in the considered system calmagite-*Zilla spinosa*, in which some physical alterations could occur [28].

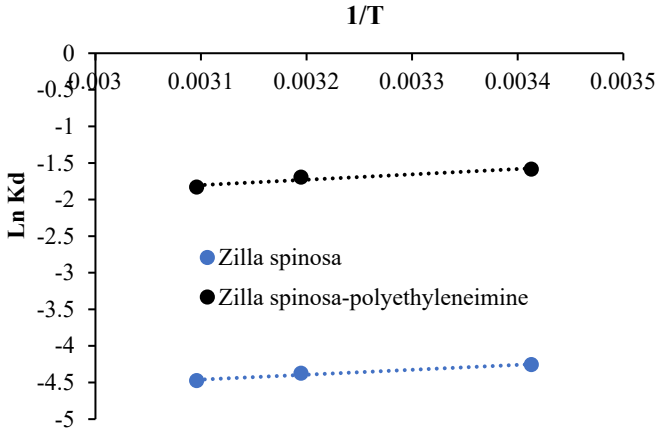

Figure 12. Plots showing the variation of Ln Kd versus 1/T for the adsorption of calmagite using virgin *Zilla spinosa* and *Zilla spinosa*-polyethyleneimine.

4. Conclusions

In this work, *Zilla spinosa* fruit was studied for the first time as an adsorbent and chemically modified with polyethyleneimine polymer. The samples were analyzed using FT-IR, SEM, XPS, and TGA techniques and further used as promising adsorbents for anionic dyes. The adsorption characteristics of the functionnalized *Zilla spinosa* fruit were investigated particularly toward calmagite, an azoic anionic dye. The adsorption capacity increased with polyethyleneimine content and achieved its maximum when the content of the polymer was equal to 5%. The adsorption capacity for *Zilla spinosa*-polyethtleneimine (5%) was equal to 114 mg/g at the following conditions: pH = 5, T = 20 °C, and time = 60 min, while it was 8.4 mg/g for the virgin *Zilla spinosa*. The adsorption followed both the pseudo-first-order and pseudo-second-order kinetic models. The interaction between *Zilla spinosa*-polyethtleneimine and calmagite is principally a physicochemical one. It was shown that the adsorption capacity of calmagite was affected by many experimental factors. The cellulosic *Zilla spinosa* fruit could interact with polyethyleneimine through electrostatic interaction or hydrogen bonds. The resulting formed complex could react with the anionic sulfonate groups of the calmagite dye through ionic interaction or also through hydrogen bonds due to the presence of hydroxyl groups in the chemical structure of the studied dye. Based on isotherms investigation, the active adsorption sites could be homogeneously distributed on the surface of the studied adsorbents. The adsorption mechanism was exothermic and non-spontaneous. Overall, it has been demonstrated that *Zilla spinosa*-polyethyleneimine was an excellent adsorbent for color from contaminated waters. As nature is rich in many biomaterials which could originate from either agriculture or marine sources, efforts will continue to valorize such abundant and available matter in many applications, including medicine, nanotechnology, water treatment, etc. Future investigations will be undertaken to explore other biomaterials for new environmental purposes.

Author Contributions: Conceptualization, M.J., A.E. and A.A.; methodology, M.J., A.E. and A.A.; software, M.J., A.E. and A.A.; data curation, M.J., A.E. and A.A.; writing—original draft, M.J.; writing—review and editing, M.J., A.A. and A.A. All authors have read and agreed to the published version of the manuscript.

Funding: The authors would like to thank the Deanship of Scientific Research at Majmaah University for supporting this work under Project No. R-2023-394.

Data Availability Statement: Not applicable.

Acknowledgments: The authors would like to thank the Deanship of Scientific Research at Majmaah University for supporting this work under Project No. R-2023-394.

Conflicts of Interest: The authors declare no conflict of interest.

References

1. Aziz, T.; Farid, A.; Chinnam, S.; Haq, F.; Kiran, M.; Alothman, Z.A.; Aljuwayid, A.M.; Habila, M.A.; Akhtar, M.S. Synthesis, characterization and adsorption behavior of modified cellulose nanocrystals towards different cationic dyes. *Chemosphere* **2023**, *321*, 137999. [CrossRef]
2. Biswal, A.K.; Sahoo, M.; Suna, P.K.; Panda, L.; Lenka, C.; Misra, P.K. Exploring the adsorption efficiency of a novel cellulosic material for removal of food dye from water. *J. Mol. Liq.* **2022**, *350*, 118577. [CrossRef]
3. Saad, E.M.; Elshaarawy, R.F.; Mahmoud, S.A.; El-Moselhy, K.M. New *Ulva lactuca* Algae Based Chitosan Bio-composites for Bioremediation of Cd(II) Ions. *J. Bioresour. Bioprod.* **2021**, *6*, 223–242. [CrossRef]
4. Obey, G.; Adelaide, M.; Ramaraj, R. Biochar derived from non-customized matamba fruit shell as an adsorbent for wastewater treatment. *J. Bioresour. Bioprod.* **2022**, *7*, 109–115. [CrossRef]
5. Ma, X.; Zhao, S.; Tian, Z.; Duan, G.; Pan, H.; Yue, Y.; Li, S.; Jian, S.; Yang, W.; Liu, K.; et al. MOFs meet wood: Reusable magnetic hydrophilic composites toward efficient water treatment with super-high dye adsorption capacity at high dye concentration. *Chem. Eng. J.* **2022**, *446*, 136851. [CrossRef]
6. Wang, B.; Lan, J.; Bo, C.; Gong, B.; Ou, J. Adsorption of heavy metal onto biomass-derived activated carbon: Review. *RSC Adv.* **2023**, *13*, 4275–4302. [CrossRef]
7. Elewa, A.M.; Amer, A.A.; Attallah, M.F.; Gad, H.A.; Al-Ahmed, Z.A.M.; Ahmed, I.A. Chemically Activated Carbon Based on Biomass for Adsorption of Fe(III) and Mn(II) Ions from Aqueous Solution. *Materials* **2023**, *16*, 1251. [CrossRef] [PubMed]
8. Jiang, D.; Li, H.; Cheng, X.; Ling, Q.; Chen, H.; Barati, B.; Yao, Q.; Abomohra, A.; Hu, X.; Bartocci, P. A mechanism study of methylene blue adsorption on seaweed biomass derived carbon: From macroscopic to microscopic scale. *Process Saf. Environ. Prot.* **2023**, *172*, 1132–1143. [CrossRef]
9. Cao, X.; Zhu, B.; Zhang, X.; Dong, H. Polymyxin *B* immobilized on cross-linked cellulose microspheres for endotoxin adsorption. *Carbohydr. Polym.* **2016**, *136*, 12. [CrossRef] [PubMed]
10. Dong, Z.; Du, J.; Wang, A.; Yang, X.; Zhao, L. Removal of methyl orange and acid fuschin from aqueous solution by guanidinium functionalized cellulose prepared by radiation grafting. *Radiat. Phys. Chem.* **2022**, *198*, 110290. [CrossRef]
11. Waly, A.I.; Khedr, M.A.; Ali, H.M.; Ahmed, I.M. Application of amino-functionalized cellulose-poly(glycidyl methacrylate) graft copolymer (AM-Cell-g-PGMA)adsorbent for dyes removal from wastewater. *Clean. Eng. Technol.* **2022**, *6*, 100374. [CrossRef]
12. Misra, N.; Rawat, S.; Goel, N.K.; Shelkar, S.A.; Kumar, V. Radiation grafted cellulose fabric as reusable anionic adsorbent: A novel strategy for potential large-scale dye wastewater remediation. *Carbohydr. Polym.* **2020**, *249*, 116902. [CrossRef] [PubMed]
13. Jawad, A.H.; Abdulhameed, A.S.; Mastuli, M.S. Acid-factionalized biomass material for methylene blue dye removal: A comprehensive adsorption and mechanism study. *J. Taibah Univ. Sci.* **2020**, *14*, 305–313. [CrossRef]
14. Sebeia, N.; Jabli, M.; Ghith, A.; Elghoul, Y.; Alminderej, F.M. Production of cellulose from *Aegagropila Linnaei* macro-algae: Chemical modification, characterization and application for the bio-sorptionof cationic and anionic dyes from water. *Int. J. Biol. Macromol.* **2019**, *135*, 152–162. [CrossRef]
15. Jabli, M.; Tka, N.; Salman, G.A.; Elaissi, A.; Sebeia, N.; Hamdaoui, M. Rapid interaction, in aqueous media, between anionic dyes and cellulosic Nerium oleander fibers modified with Ethylene-Diamine and Hydrazine. *J. Mol. Liq.* **2017**, *242*, 272–283. [CrossRef]
16. Tka, N.; Jabli, M.; Saleh, T.A.; Salman, G.A. Amines modified fibers obtained from natural Populus tremula and their rapid biosorption of Acid Blue 25. *J. Mol. Liq.* **2018**, *250*, 423–432. [CrossRef]
17. Farahat, E.; Linderholm, H.W. Linderholm. Effects of treated wastewater irrigation on size-structure, biochemical products and mineral content of native medicinal shrubs. *Ecol. Eng.* **2013**, *60*, 235–241. [CrossRef]
18. Al-Qahtani, H.; Alfarhan, A.H.; Al-Othman, Z.M. Changes in chemical composition of *Zilla spinosa* Forssk. medicinal plants grown in Saudi Arabia in response to spatial and seasonal variations. *Saudi J. Biol. Sci.* **2020**, *27*, 2756–2769. [CrossRef]
19. Feng, Y.; Liu, Y.; Xue, L.; Sun, H.; Guo, Z.; Zhang, Y.; Yang, L. Carboxylic acid functionalized sesame straw: A sustainable cost-effective bio adsorbent with superior dye adsorption capacity. *Bioresour. Technol.* **2017**, *238*, 675–683. [CrossRef]
20. Oliveira, R.N.; Mancini, M.C.; Oliveira, F.C.S.; Passos, T.M.; Quility, B.; Thire, R.M.S.; Mcguiness, G.B. FTIR analysis and quantification of phenols and flavonoids of five commercially available plants extracts used in wound healing. *Rev. Matéria* **2016**, *21*, 767–779. [CrossRef]

21. Poletto, M.; Zattera, A.J.; Santana, R.M.C. Structural differences between wood species: Evidence from chemical composition, FTIR spectroscopy, and thermogravimetric analysis. *J. Appl. Polym. Sci.* **2012**, *126*, E337–E344. [CrossRef]
22. Chen, X.; Xu, R.; Xu, Y.; Hu, H.; Pan, S.; Pan, H. Natural adsorbent based on sawdust for removing impurities in waste lubricants. *J. Hazard. Mater.* **2018**, *350*, 38–45. [CrossRef] [PubMed]
23. Yang, H.; Yan, R.; Chen, H.; Lee, D.H.; Zheng, C. Characteristics of hemicellulose, cellulose and lignin pyrolysis. *Fuel* **2007**, *86*, 1781–1788. [CrossRef]
24. Jiang, F.; Hsieh, Y.L. Chemically and mechanically isolated nanocellulose and their self-assembled structures. *Carbohydr. Polym.* **2013**, *95*, 32–40. [CrossRef] [PubMed]
25. Oun, A.A.; Rhim, J.W. Isolation of oxidized nanocellulose from rice straw using the ammonium persulfate method. *Cellulose* **2018**, *25*, 2143–2149. [CrossRef]
26. Nasuha, N.; Hameed, B.H.; Din, A.T. Rejected tea as a potential low-cost adsorbent for the removal of methylene blue. *J. Hazard. Mater.* **2010**, *175*, 126–132. [CrossRef] [PubMed]
27. Gucek, A.; Sener, S.; Bilgen, S.; Mazmanci, A. Adsorption and kinetic studies of cationic and anionic dyes on pyrophyllite from aqueous solutions. *J. Coll. Interf. Sci.* **2005**, *286*, 53–60. [CrossRef]
28. Ho, Y.S.; McKay, G. Pseudo-second order model for sorption processes. *Process Biochem.* **1999**, *34*, 451–465. [CrossRef]
29. Guo, J.-Z.; Li, B.; Liu, L.; Lv, K. Removal of methylene blue from aqueous solutions by chemically modified bamboo. *Chemosphere* **2014**, *111*, 225–231. [CrossRef]
30. Treybal, R.E. *Mass-Transfer Operations*, 3rd ed.; McGraw-Hill: New York, NY, USA, 1981.